



Research article

Differential expression profiles and bioinformatics analysis of tRNA-derived small RNAs in epicardial fat of patients with atrial fibrillation

Feng Jiang¹, Lingling Qin, Yidan Wang, Yuanshu Peng, Liping Yu, Pixiong Su, Lei Zhao^{*,1}

Heart Center & Beijing Key Laboratory of Hypertension, Beijing Chaoyang Hospital, Capital Medical University, Beijing, 100020, China

ARTICLE INFO

Keywords:

Atrial fibrillation
Epicardial fat
tRFs & tRNAs
Sequencing
Bioinformatics

ABSTRACT

The exact processes underlying atrial fibrillation (AF) are still unclear. It has been suggested that epicardial adipose tissue (EAT) may contribute to arrhythmias and can release various bioactive molecules, including exosomes containing tRNA-derived small RNAs (tsRNAs). Numerous studies have indicated that these tsRNAs can significantly affect key cellular functions. However, there is currently no research investigating the relationship between tsRNAs from EAT and AF. In order to explore the regulatory mechanisms of tsRNAs from EAT associated with AF, we conducted RNA-sequencing analysis on EAT samples collected from 6 AF patients and 6 control subjects with sinus rhythm. Our analysis revealed an upregulation of 146 tsRNAs and a downregulation of 126 tsRNAs in AF. Furthermore, we randomly selected four tsRNAs (tRF-Sec-TCA-001, tRNA-Gly-CCC-003, tRF-Gly-GCC-002, and tRF-Tyr-GTA-007) for validation using quantitative reverse transcription-polymerase chain reaction. Following this, bioinformatic analyses revealed that the target genes of these tsRNAs were prominently involved in the regulation of cell adhesion and various cellular processes mediated by plasma membrane adhesion molecules. Additionally, based on KEGG analysis, it was suggested that the majority of these target genes might contribute to the pathogenesis of AF through processes such as glycosaminoglycan biosynthesis, AMP-activated protein kinase activity, and the insulin signaling pathway. Our results elucidate changes in the expression profiles of tsRNAs within EAT samples obtained from AF patients, and they forecast potential target genes and interactions between tsRNAs and mRNA within EAT that could contribute to the pathogenesis of AF.

1. Introduction

Atrial fibrillation (AF) is the most common sustained arrhythmia and is associated with an increased risk of serious complications, including ischaemic stroke, dementia and heart failure, resulting in significant morbidity and mortality [1]. To date, advancements in our understanding of AF pathophysiology have catalyzed substantial strides in therapeutic strategies, such as catheter ablation.

* Corresponding author. Heart Center & Beijing Key Laboratory of Hypertension, Beijing Chaoyang Hospital, Capital Medical University, Beijing, 100020, China.

E-mail address: lily885300@sina.com (L. Zhao).

¹ These authors contributed equally to this work.

<https://doi.org/10.1016/j.heliyon.2024.e30295>

Received 24 July 2023; Received in revised form 23 April 2024; Accepted 23 April 2024

Available online 26 April 2024

2405-8440/© 2024 The Authors. Published by Elsevier Ltd. This is an open access article under the CC BY-NC license (<http://creativecommons.org/licenses/by-nc/4.0/>).

However, the multifactorial etiology of AF presents challenges in delineating potential molecular biomarkers associated with structural and electronic remodelling [2], autonomic nervous dysfunction and calcium dysregulation [2]. Consequently, elucidating the mechanism of AF and exploring innovative therapeutic modalities remain imperative pursuits.

There is robust evidence showing a close association between obesity and a high risk of AF. Visceral adipose tissue is believed to provide a structural (typically fibrotic) substrate for atrial remodelling and participate in the trigger and maintenance of AF [1,3]. Epicardial adipose tissue (EAT), situated within the atrioventricular and interventricular grooves of the heart, represents a cardiac visceral fat depot that has garnered significant scientific attention owing to its close proximity to the myocardium [4,5]. Epicardial adipose tissue (EAT) is increasingly acknowledged for its metabolic activity and hypothesized arrhythmogenic potential. Moreover, it serves as a source of diverse bioactive molecules, including exosomes harboring small noncoding RNAs (sncRNAs), which are postulated to exert paracrine effects on the atrial myocardium. Transfer RNAs (tRNAs) are sncRNAs and mainly participate in protein synthesis [6]. tRNA-derived small RNAs (tsRNAs), originating from tRNAs through specific cleavage events, represent a heterogeneous class characterized by lengths ranging from 18 to 40 nucleotides. Their initial identification occurred in the urine specimens of individuals diagnosed with cancer [7,8]. The advent of high-throughput sequencing technology has facilitated the identification of an expanding repertoire of tsRNAs, revealing their involvement in modulating biological processes through various mechanisms including RNA silencing, ribosome biogenesis, retrotransposition, and epigenetic inheritance [9]. Additionally, approximately 45 % of tsRNAs have been detected in extracellular vesicles, selectively released from T cells via multivesicular bodies, potentially influencing immunosuppressive mechanisms [10]. Furthermore, compared with plasma tsRNAs, circulating exosomal tsRNAs show greater potential as biomarkers in large-artery atherosclerotic stroke [11]. The bilayers of vesicle may isolate exosomal tsRNAs from biological enzymes in plasma, which makes it more stable.

Generally, depending on the cleavage location on tsRNAs, tsRNAs can be divided into two species: tRNA-derived fragments (tRFs) and tRNA-derived stress-induced RNAs (tiRNAs). tRFs are close in length to microRNAs (miRNAs) and can be classified into four subclasses: tRF-1, tRF-3, tRF-5 and i-tRF. Under conditions of stress, such as hypoxia, UV radiation, and oxidative stress, tiRNAs are generated as tRNA half-molecules through specific cleavage mediated by angiogenin [12]. Recent research suggests that these particular tsRNAs are not randomly generated through tRNA cleavage, but instead possess diverse biological functions and dynamically influence fundamental cellular processes, including embryogenesis and the pathogenesis of various cancers [7,13]. However, as of now, no studies have uncovered the correlation between tsRNAs derived from epicardial adipose tissue (EAT) and atrial fibrillation (AF), leaving their interactions and potential signaling pathways yet to be elucidated. We recently reported the long noncoding RNA and mRNA profiles in EAT of patients with AF [14]. This study examined the expression profile of tsRNAs, and we hypothesized that tsRNAs may participate in atrial remodelling by acting as miRNAs and targeting mRNAs in different ways.

Therefore, the aim of this study was to describe the tsRNA spectrum in EAT of AF and determine the mechanisms behind tRFs and tiRNAs of EAT in AF. The research design of this study is presented in Fig. 1.

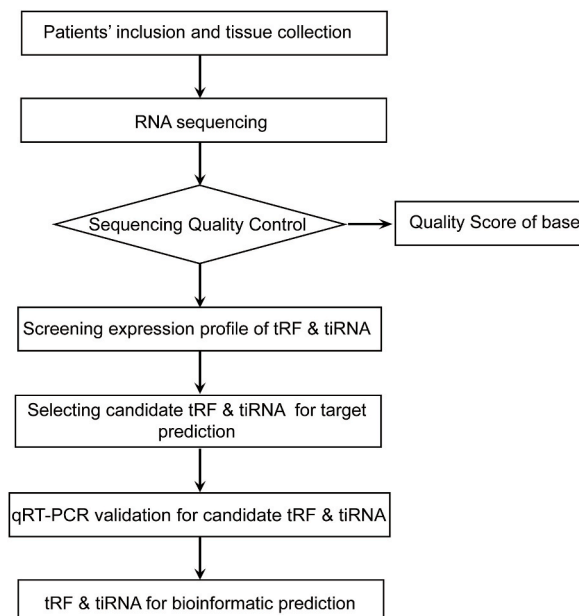


Fig. 1. Study design illustration. qRT-PCR, quantitative reverse transcription-polymerase chain reaction.

2. Materials and methods

2.1. Study participants and samples

The study adhered to the principles outlined in the 1975 Declaration of Helsinki and obtained approval from the Ethical Committee of Beijing Chaoyang Hospital (2021-ke-246). The enrolled patients provided written informed consent. In the study, consecutive patients who underwent coronary artery bypass grafting in the Department of Heart Center were recruited. EAT samples were collected from patients with persistent nonvalvular AF (n = 6) and from patients in sinus rhythm (SR) (n = 6). Persistent AF was defined as a sustained episode lasting more than 7 days. Epicardial biopsy specimens (1–2 cm³ in volume) were acquired prior to the onset of cardiopulmonary bypass, precisely from the atrioventricular groove. Subsequently, the collected samples were fragmented, rinsed with phosphate-buffered saline (PBS), promptly cryopreserved in liquid nitrogen, and ultimately preserved at –80 °C until subsequent RNA extraction procedures.

2.2. RNA extraction and quality control

Total RNA was extracted from frozen EAT specimens using the QIAGEN miRNeasy Mini Kit (Qiagen, Hilden, Germany) following the manufacturer's protocol. The integrity and concentration of RNA samples underwent quality control (QC) assessments prior to sequencing. QC procedures included agarose gel electrophoresis and spectrophotometric analysis using a Nanodrop 1000 instrument (Thermo Scientific, Wilmington, DE).

2.3. tRF & tiRNA pretreatment and library preparation

Total RNA samples underwent pretreatment to remove RNA modifications that could impede library construction, as described below: 3'-aminoacyl (charged) deacylation to 3'-OH for 3' adaptor ligation, 3'-cP (2',3''-cyclic phosphate) removal to 3'-OH for 3' adaptor ligation, 5'-OH (hydroxyl group) phosphorylation to 5'-P for 5'-adaptor ligation, and m1A and m3C demethylation for efficient reverse transcription. Then, pretreated total RNA was used to prepare the sequencing library. First, total RNA was ligated to 3' and 5' small RNA adapters. Then, cDNA was synthesized and amplified using Illumina's proprietary RT primers and amplification primers. Third, 134–160 bp amplified fragments were purified from the PAGE gel, and finally, the complete libraries were quantified by an Agilent 2100 Bioanalyzer (Invitrogen, USA).

2.4. Sequencing of tRFs & tiRNAs

Diluted libraries were subjected to denaturation to produce single-stranded DNA molecules, followed by sequencing for 50 cycles using an Illumina NextSeq 500 system equipped with a NextSeq 500/550 V2 kit (#FC-404-2205, Illumina).

2.5. Data analysis of tRFs & tiRNAs

Solexa pipeline v1.8 software was used for image analysis and base calling. Sequencing quality was examined by FastQC. The abundance of tRFs and tiRNAs was calculated using sequencing counts and normalized as counts per million total aligned reads (CPM). The differential expression profiles of tRFs and tiRNAs were evaluated based on the count value with edgeR. Principal component analysis (PCA), Venn Diagram, Hierarchical clustering and Scatter/Volcano Plots were generated in R.

2.6. Bioinformatic prediction and functional enrichment analysis of tRFs and tiRNAs

Prediction of targets of candidate tsRNAs was performed using TargetScan and miRanda, and the results were visualized using Cytoscape. Furthermore, to determine the possible biological function of differentially expressed tRFs and tiRNAs, we carried out Gene Ontology (GO) enrichment analysis (<http://www.geneontology.org>) and Kyoto Encyclopedia of Genes and Genomes (KEGG) pathway analysis (<http://www.genome.jp/kegg>). In GO enrichment analysis, biological processes (BPs), molecular functions (MFs) and cellular components (CCs) were identified to elucidate potential signalling clusters encompassing the differentially expressed targets.

2.7. Validation with quantitative real-time PCR

Quantitative real-time PCR was applied to confirm candidate tsRNA sequencing results. Total RNA extraction was performed utilizing the QIAGEN miRNeasy Mini Kit (Qiagen, Hilden, Germany), followed by cDNA synthesis employing the rtStar™ tRFs & tiRNAs Pretreatment Kit (Arraystar) in conjunction with the rtStar™ First Strand cDNA Synthesis Kit (Arraystar). Subsequent PCR amplification was conducted utilizing the ViiA 7 Real-time PCR system (Applied Biosystems), with normalization of tsRNA expression levels to U6 RNA.

2.8. Statistics

Categorical variables are depicted as frequencies and percentages, while numerical variables conforming to a normal distribution

were expressed as the mean \pm SE. For numerical variables exhibiting a skewed distribution, the median along with the 25th and 75th percentiles (P25, P75) were reported. Group comparisons were conducted utilizing independent-sample t-tests for continuous variables and chi-square or Fisher's exact tests for categorical variables. Clinical analysis was executed utilizing IBM SPSS Statistics 24.0, with statistical significance defined as a two-tailed P -value < 0.05 . Sequencing analysis, encompassing Venn diagrams, hierarchical clustering, and GO/KEGG pathway analyses, was conducted employing the R programming package. PCA was employed to reduce dataset dimensionality and examine sample classification based on expression profiles. Differential expression analysis of tRFs and tiRNAs was conducted utilizing the R programming package, employing a fold change threshold of > 1.5 and a significance threshold of $P < 0.05$ for screening purposes.

3. Results

3.1. Differential expression of tRFs & tiRNAs

This study investigated the expression profile of transcriptomes of epicardial fat depots in AF ($n = 6$) and SR ($n = 6$) subjects by high-throughput RNA sequencing. The baseline characteristics and clinical parameters are detailed in Supplemental Table 1 and the quality score plot of each sample is outlined in Table 1. Q30 means 99.9 % base calling accuracy, and as shown in Table 1, a larger proportion of bases in each sample achieved Q30 (more than 90 %). Additionally, the PCA plot in the study showed distinguishable tRF and tiRNA expression profiles (Fig. 2A).

Overall, a total of 473 tsRNAs were differentially expressed, among which 146 tsRNAs were upregulated in AF, while 126 were downregulated. The distinguishable tRF and tiRNA expression profile and variation between AF and SR were shown in Fig. 2B–D, and the experimental data on the top 20 upregulated and downregulated tsRNAs are detailed in Table 2.

In Fig. 3A, the Venn diagram shows that 206 tsRNAs were shared in both groups, while 80 tsRNAs were uniquely expressed in the AF group and 8 were uniquely expressed in the SR group. Seventy tsRNAs were identified from the tRF database (Fig. 3B). In the pie chart, the distribution of the number of subtype tRFs and tiRNAs was graphed (with an average CPM greater than 20). In comparison to the SR group, notable increases were observed in the expression levels of tiRNA-5, tRF-1, tRF-3a, tRF-3b and tRF-5a, while tRF-5c levels exhibited a significant decrease (Fig. 3C and D). The stacked bar charts depicted in Fig. 3E and F, delineating the distribution of tsRNA subtypes across tRNA isodecoders, and the frequency distribution with respect to length, as illustrated in Fig. 3G and H, highlight marked discrepancies in subtype distribution between the two groups.

3.2. Validation by qRT-PCR

In order to validate the credibility of the high-throughput sequencing data, four prospective tsRNAs (tRF-SeC-TCA-001, tiRNA-Gly-CCC-003, tRF-Gly-GCC-002, and tRF-Tyr-GTA-007) were selected at random for qRT-PCR. Compared with the control, tRF-SeC-TCA-001 and tiRNA-Gly-CCC-003 had significantly increased expression levels, while tRF-Gly-GCC-002 and tRF-Tyr-GTA-007 were downregulated in AF, which is consistent with the sequencing results (Fig. 4).

3.3. Predicted targets by bioinformatics analysis

The four candidate tsRNAs with differential expression were further analyzed using bioinformatics tools such as TargetScan and miRanda for prediction. According to the tsRNA-target network, a total of 2672 target genes were reported to be associated with these candidate tsRNAs. We developed a network illustrating the interaction between tsRNAs and mRNA, incorporating the top 100

Table 1
Quality score.

Sample	Total Read	Total Base	BaseQ30	Base30 (%)
AF-1	10539403	537509553	501738225	93.34
AF-2	9126561	465454611	432399080	92.90
AF-3	9105223	464366373	433205005	93.29
AF-4	11392677	581026527	542860679	93.43
AF-5	9407894	479802594	448164130	93.41
AF-6	7420499	378445449	353930856	93.52
SR-1	8760739	446797689	416639194	93.25
SR-2	10260164	523268364	490239587	93.69
SR-3	8589294	438053994	406931685	92.90
SR-4	8804405	449024655	419726053	93.48
SR-5	8484260	432697260	404635018	93.51
SR-6	9402354	479520054	447081561	93.24

AF: Atrial fibrillation; SR: Sinus rhythm.

Total Read: Raw sequencing reads after quality filtering.

Total Base: Number of bases after quality filtering.

BaseQ30: Number of bases of Q score more than 30 after quality filtering.

BaseQ30(%): The proportion of bases ($Q \geq 30$) number after quality filtering.

Table 2
Top 20 up- and down-regulated tsRNAs in epicardial adipose tissue of atrial fibrillation.

tRF_ID	Type	Length	Fold Change	P Value	Regulation
tRF-SeC-TCA-001	tRF-5a	15	60.355	0.000005	Up
tRF-Ser-CGA-006	tRF-5a	16	24.571	0.000099	Up
tRF-SeC-TCA-007	tRF-5a	14	16.057	0.000908	Up
tRF-Trp-TCA-001	tRF-3b	19	10.817	0.002756	Up
tiRNA-Gly-CCC-003	tiRNA-5	33	10.607	0.000440	Up
tRF-Leu-AAG-003	tRF-5a	16	9.527	0.000019	Up
tiRNA-Lys-CTT-005	tiRNA-5	34	8.886	0.000052	Up
tiRNA-Lys-CTT-001	tiRNA-5	34	8.333	0.000192	Up
tRF-Ser-TGA-032	tRF-5a	15	8.077	0.000243	Up
tRF-Leu-TAG-002	tRF-5a	16	7.552	0.000045	Up
tRF-Tyr-GTA-014	tRF-5a	14	7.042	0.001284	Up
tRF-Gly-TCC-034	tRF-1	14	6.880	0.000779	Up
tiRNA-Lys-CTT-003	tiRNA-5	34	6.763	0.000681	Up
tiRNA-Gln-CTG-003	tiRNA-5	34	6.523	0.004188	Up
tiRNA-Val-TAC-002	tiRNA-5	34	6.217	0.000323	Up
tiRNA-Lys-CTT-002	tiRNA-5	34	6.176	0.000388	Up
tRF-Ser-TGA-011	tRF-5a	16	6.106	0.003426	Up
tRF-Leu-CAA-002	tRF-5a	15	6.034	0.000919	Up
tRF-Leu-AAG-002	tRF-5a	15	5.809	0.000248	Up
tRF-Leu-CAA-003	tRF-5a	16	5.772	0.000262	Up
tRF-Cys-GCA-082	tRF-1	23	0.004	0.013645	Down
tRF-Gly-GCC-002	tRF-5c	28	0.136	0.008148	Down
tRF-Tyr-GTA-011	tRF-3a	18	0.138	0.001427	Down
tRF-Ser-TGA-028	tRF-1	16	0.159	0.000224	Down
tRF-Tyr-GTA-007	tRF-3a	18	0.172	0.001083	Down
tRF-Gly-CCC-033	tRF-5c	28	0.173	0.002105	Down
tRF-Tyr-GTA-006	tRF-3a	17	0.190	0.004556	Down
tRF-Tyr-GTA-010	tRF-3a	18	0.197	0.002557	Down
tRF-Gln-TTG-006	tRF-5b	22	0.227	0.003141	Down
tRF-Gly-GCC-007	tRF-5c	28	0.229	0.012558	Down
tRF-Gly-GCC-008	tRF-5c	29	0.230	0.021273	Down
tiRNA-Met-CAT-001	tiRNA-5	31	0.233	0.032961	Down
tRF-Tyr-GTA-005	tRF-3a	17	0.234	0.004964	Down
tRF-Gly-CCC-011	tRF-5c	29	0.236	0.026977	Down
tRF-Gly-GCC-029	tRF-5c	29	0.238	0.020842	Down
tRF-His-GTG-047	tRF-1	28	0.239	0.009419	Down
tRF-Val-CAC-001	tRF-3a	17	0.248	0.0042	Down
tRF-Gly-CCC-010	tRF-5c	28	0.249	0.021616	Down
tRF-Val-CAC-046	tRF-3a	18	0.252	0.019431	Down
tRF-Gly-GCC-010	tRF-5c	31	0.266	0.014524	Down

especially their crucial roles in the development of various tumours [7], few studies have investigated the association between tsRNAs and AF pathogenesis. In this investigation, we elucidated a comprehensive profile of tRFs and tiRNA in human EAT associated with AF through small RNA sequencing. Furthermore, bioinformatic analyses indicated the potential regulatory role of tsRNAs in the pathophysiological processes mediated by the AMPK and insulin signaling pathways. To our knowledge, this study represents the initial comprehensive examination of tsRNA expression within human EAT, elucidating its role in AF pathogenesis. Additionally, the functional annotation of predicted targets offers novel insights into potential pathways implicated in AF pathophysiology.

Due to their prevalence within cells and robust stability, tsRNAs have traditionally been regarded as exhibiting a relatively high degree of conservation. However, it is becoming increasingly clear that changes in their abundance or nucleotide modification might lead to aberrant translation and a shift in disease status. Accumulating evidence reveals that tsRNAs contribute to viral infection, tumours, neurodegeneration and metabolic dysfunction. In the context of viral infections, sncRNAs are integral to modulating host immunity, orchestrating host-viral interactions, and regulating viral replication [15,16]. Viruses can improve their replication and efficiency in infection by exploiting host tRFs as guide primers. Zhou et al. revealed that respiratory syncytial virus (RSV) specifically induces the novel production of tRF-5^{GlyCCC} and tRF-5^{LysCTT}, both of which contribute to RSV replication and cascade effects of cytokines and chemokines [16]. Furthermore, the sncRNA profile in human nasopharyngeal swab samples was found to change, and among these impacted ncRNAs, tRFs were the most significantly affected in SARS-CoV-infected airway epithelial cells [17]. In gastric cancer, tRF-3017A (derived from tRNA-Val-TAC) silences the tumour suppressor gene and prompts lymph node metastasis [18]. In addition, both tRFs and tiRNAs have emerged as novel biomarkers for assessing therapeutic efficacy in skin melanoma [19,20]. Regarding neurodegenerations, WW. and colleagues observed that tRFs were significantly altered in the hippocampus of Alzheimer's disease patients, and the methylation sites of tRNAs determined disease progression in these stress-induced neurodevelopmental disorders [21]. Additionally, angiogenin-mediated biogenesis of 5'-tsRNAs in sperm was reported to contribute to paternal inflammation-induced metabolic disorders in offspring [22]. To date, there exists no prior investigation into the profiling of tsRNA expression within EAT linked to AF. However, a study has reported altered tsRNA expression in rheumatic heart disease with AF, utilizing cardiac papillary muscles as sample material [23]. Consequently, following sequencing and subsequent bioinformatic

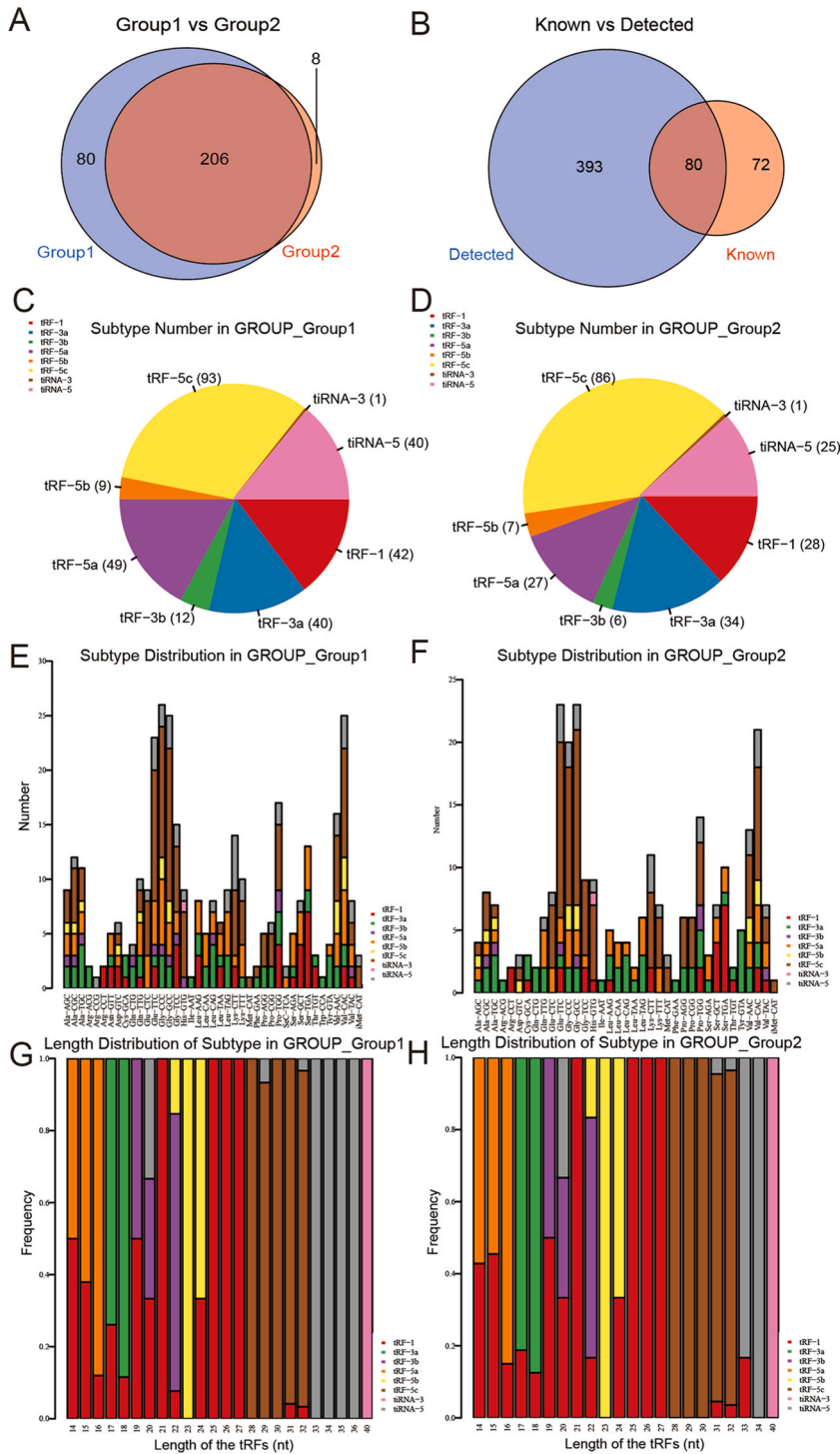


Fig. 3. Analysis of tsRNA subtypes. (A) Venn diagram based on the number of commonly and specifically expressed tRFs and tIRNs. (B) Venn diagram based on the number of known and detected tRFs and tIRNs. (C–D) Pie charts of the distribution of subtypes of tRFs & tIRNs of epicardial adipose tissue in atrial fibrillation (C) and sinus rhythm (D). (E–F) The number of subtypes of tRFs and tIRNs against tRNA isodecoders in the two groups. (G–H) The frequency of subtype versus length of tRFs and tIRNs in the two groups.

analysis, our study revealed a notable finding: the expression levels of tsRNAs within the human EAT were significantly altered in the presence of AF compared to SR. In this investigation, the analysis of tsRNA subtypes against tRNA isodecoders and their frequency distribution according to length (Fig. 2) revealed a diverse landscape, suggesting that tsRNAs may represent promising candidates for

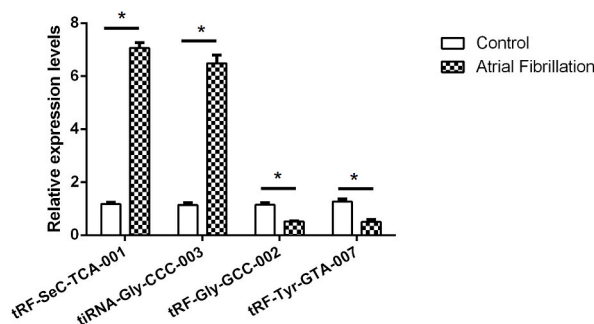


Fig. 4. Validation by qRT-PCR in human epicardial adipose tissue of atrial fibrillation and control. AF, atrial fibrillation. Mean \pm SEM (n = 6). *P < 0.05.

modulating atrial substrates in the context of AF.

TsRNAs are derived fragments sliced from tRNAs, and similar to miRNAs, tsRNAs bind to corresponding sequences in mRNAs and regulate target gene expression at a posttranslational level. Utilizing the miRNA-like mechanisms exhibited by these molecules, we employed bioinformatics methodologies to predict potential mRNA targets for candidate tsRNAs and subsequently established an interactive network depicting the interactions between tsRNAs and their putative mRNA targets. The target genes identified by GO enrichment analysis were mainly involved in cell adhesion and cellular processes via plasma membrane adhesion molecules.

In the KEGG pathway analysis, glycosaminoglycan biosynthesis, the AMPK and insulin signalling pathways were the top three signalling pathways emerged as the top three pathways influenced by the candidate tsRNA-mRNA network. It has been reported that failing human hearts displays significant perivascular and interstitial chondroitin sulfate glycosaminoglycans (CS-GAGs) accumulation, particularly in region of intense fibrosis. Tumor necrosis factor- α , which induced inflammation gene activation in vitro in endothelial cells and macrophages, was identified as a direct binding partner of CS-GAGs [24]. Andreas Haryono [25] pointed out that CS-GAGs might have biphasic effects on cardiac function and remodelling in heart failure since CS-GAGs protect cardiomyocyte from acute injury stress; therefore, stage-dependent approaches for CS-GAGs-targeted therapy are required to treat myocardial remodelling. AMPK plays a crucial role in maintaining electrophysiological homeostasis in the atrium. A recent study by Dan et al. reported impaired AMPK signalling in heart failure with preserved ejection fraction associated with AF [26]. Furthermore, by constructing atrium-selective cardiac AMPK deletion remodelling mice, Kevin proved the essential homeostatic role of AMPK in the atrium, which protects against electrophysiological reprogramming of atrial ion channels and gap junction proteins that might promote the development and perpetuation of AF [27]. In addition, metabolic syndrome with insulin resistance has already been proven to be a risk factor associated with the occurrence of AF and recurrence after radiofrequency catheter ablation [28]. Candidate tsRNAs may target mRNAs that regulate insulin resistance and participate in the pathology of AF.

Considering the intricate nature of AF initiation and progression, it is imperative to investigate the biological role of EAT in AF pathogenesis, particularly in relation to tsRNAs. Nonetheless, several unresolved queries persist. Firstly, while our study identified differentially expressed tsRNAs in EAT through RNA sequencing and conducted functional predictions using bioinformatics tools, further elucidation of tsRNA-mRNA interactions and functions necessitates in vitro and in vivo validation in subsequent investigations. Our analyses predominantly relied on in silico methodologies, underscoring the need for additional animal models and clinical validation to elucidate the precise involvement of tsRNAs in AF. Secondly, the study's limitations, notably the modest sample size, underscore the necessity for comprehensive secondary analyses in larger-scale studies.

In conclusion, our study presents, for the first time, the altered expression profiles of tsRNAs in epicardial adipose samples obtained from AF patients. Additionally, we have predicted potential target genes and elucidated tsRNA-mRNA interactions within EAT that may contribute to AF pathogenesis. These findings offer valuable insights for future investigations aimed at exploring innovative therapeutic strategies targeting atrial remodelling. Further research endeavors are warranted to delineate the physiological mechanisms through which these tsRNAs modulate the progression of AF.

Data availability statement

The sequencing raw data has been uploaded to Gene Expression Omnibus (GEO) (GSE210705, <https://www.ncbi.nlm.nih.gov/geo/query/acc.cgi?acc=GSE210705>).

Funding

None.

CRediT authorship contribution statement

Feng Jiang: Writing – original draft, Data curation. **Lingling Qin:** Formal analysis, Data curation. **Yidan Wang:** Formal analysis,

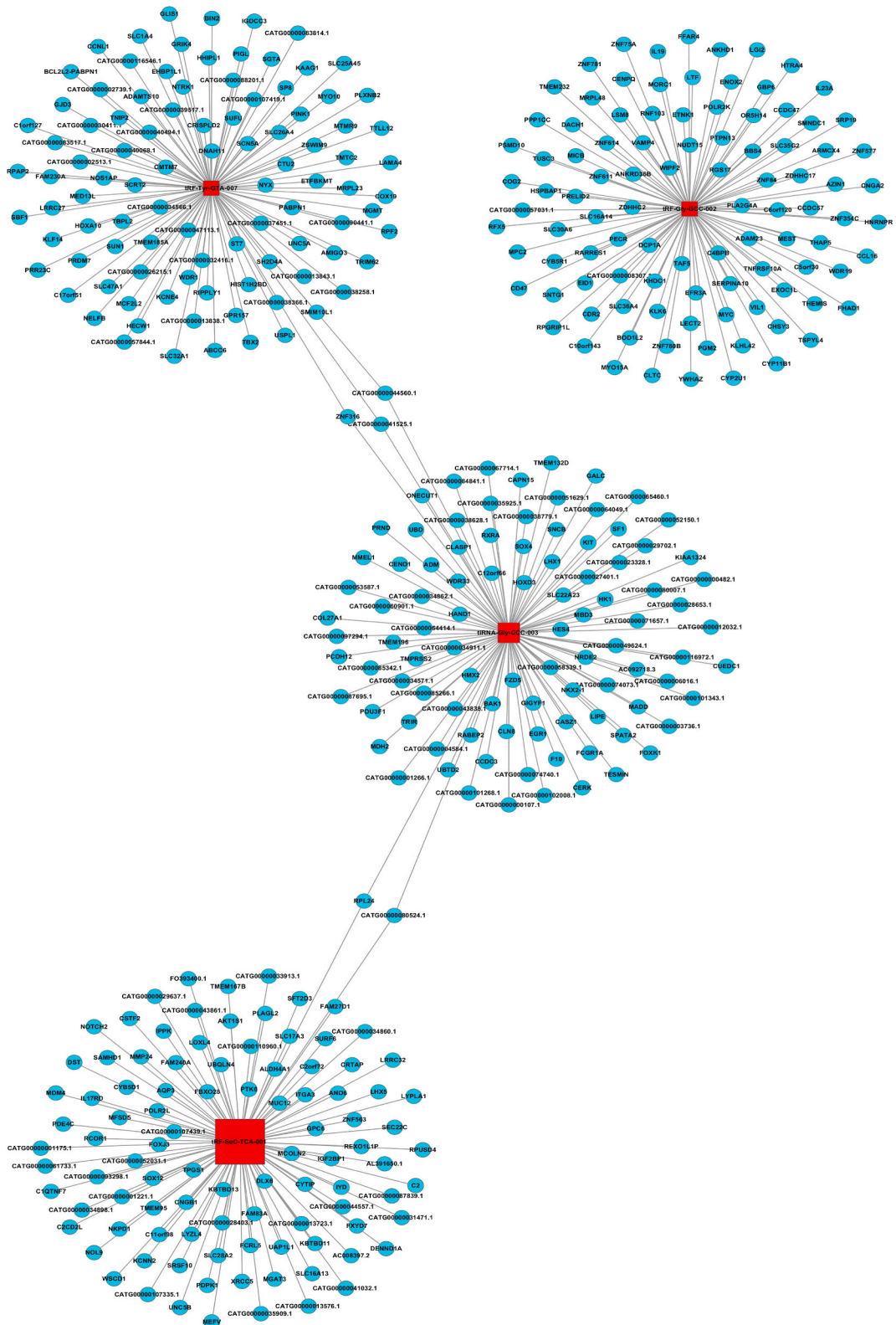


Fig. 5. The network of candidate tsRNAs and potential target mRNAs. All results have a threshold of ≥ 1.5 -fold change.

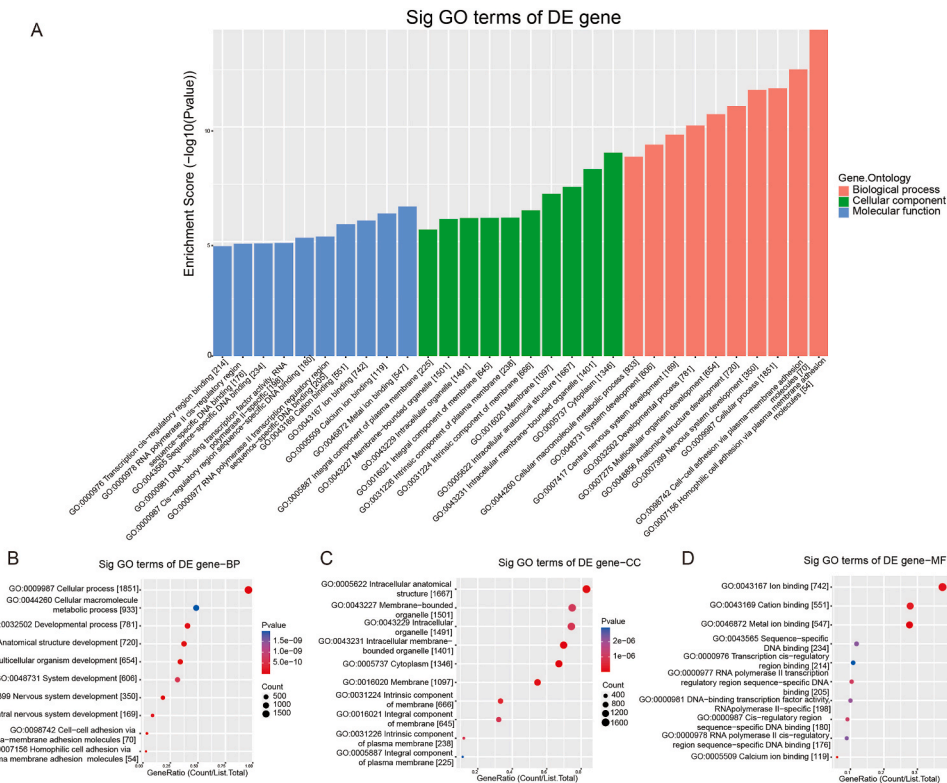


Fig. 6. GO enrichment analysis of target mRNAs of the four candidate tsRNAs. (A) Bar plot with enrichment score: top ten enriched items in three domains. (B–D) Dot plot with gene ratio values of the top ten enriched items in biological processes (B), cellular components (C) and molecular functions (D).

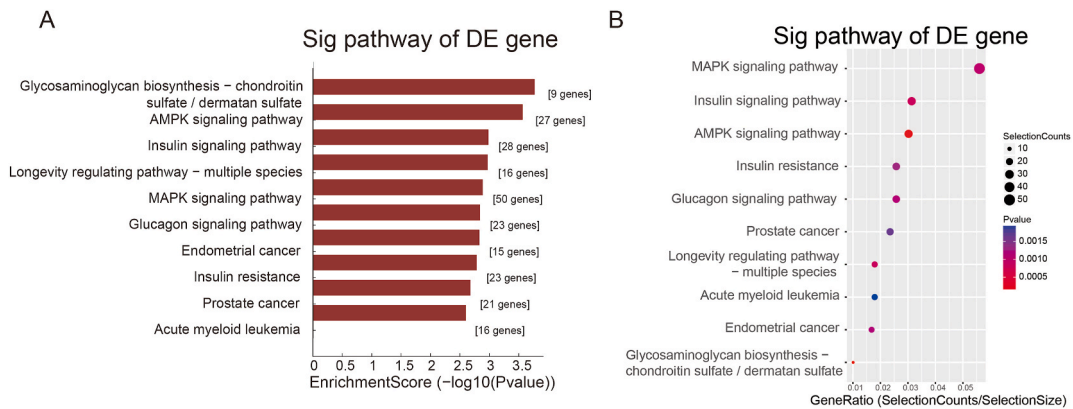


Fig. 7. KEGG pathway analysis of target mRNAs of the four candidate tsRNAs. (A) Pathway bar plot with enrichment score values of the top ten significantly enriched signalling pathways. (B) Dotplot with gene ratio values of the top ten significantly enriched signalling pathways.

Data curation. Yuanshu Peng: Methodology, Formal analysis, Data curation. Liping Yu: Project administration, Methodology. Pixiong Su: Visualization, Conceptualization. Lei Zhao: Writing – review & editing, Writing – original draft, Resources, Methodology, Conceptualization.

Declaration of competing interest

The authors declare that they have no known competing financial interests or personal relationships that could have appeared to influence the work reported in this paper.

Table 3

Top 10 KEGG pathways of differentially expressed target mRNAs based on candidate tsRNAs in epicardial adipose tissue.

Pathway	Definition	Selection Counts	P values	Genes
hsa00532	Glycosaminoglycan biosynthesis - chondroitin sulfate/dermatan sulfate	9	0.0001222909	B3GALT6//CHST11//CHST12//CHST15//CHST3//CHST7//CHSY3//DSE//XYLT1
hsa04152	AMPK signaling pathway	27	0.0001980609	ADIPOQ//AKT1//AKT1S1//CAB39//CAMKK2//CCND1//CREB1//ELAVL1//FOXO1//G6PC2//HNF4A//IRS2//IRS4//LIPE//PDPK1//PFKFB3//PFKP//PIK3CD//PPARGC1A//PPP2R2D//PPP2R5A//PPP2R5E//PRKAA2//PRKAG3//RAB10//RAB2A//RPTOR
hsa04910	Insulin signaling pathway	28	0.0008022508	AKT1//BAD//BRAF//CBLB//CRK//FOXO1//G6PC2//GRB2//HK1//IKKBK//IRS2//IRS4//LIPE//PDE3B//PDPK1//PIK3CD//PPARGC1A//PPP1CA//PPP1CC//PPP1R3A//PRKAA2//PRKACB//PRKAG3//PRKCZ//PTPN1//RPTOR//SOCS4//TRIP10
hsa04213	Longevity regulating pathway - multiple species	16	0.0008179964	ADCY1//ADCY5//AKT1//AKT1S1//CLPB//EIF4EBP2//FOXO1//HDAC2//HSPA1B//IRS2//IRS4//PIK3CD//PRKAA2//PRKACB//PRKAG3//RPTOR
hsa04010	MAPK signaling pathway	50	0.001008446	AKT1//ANGPT2//ANGPT4//ATF2//BRAF//CACNA2D1//CACNB2//CACNG8//CASP3//CHUK//CRK//CSF1R//DUSP2//DUSP6//EFNA2//EFNA3//EREG//FGF2//FGF5//FLT1//GADD45B//GADD45G//GRB2//HSPA1B//IKKBK//KIT//MAP3K1//MAPK11//MYC//NF1//NFATC3//NTRK1//NTRK2//PAK2//PDGFA//PDGFB//PDGFD//PLA2G4A//PLA2G4D//PPM1B//PPP3CB//PPP3R2//PRKACB//RASGRP3//RPS6KA2//RPS6KA3//RPS6KA5//RPS6KA6//TAB1//TAOK1
hsa04922	Glucagon signaling pathway	23	0.001123091	AKT1//ATF2//CAMK2G//CREB1//CREBBP//FOXO1//G6PC2//GNAQ//LDHAL6A//LDHAL6B//LDHB//PDE3B//PFKP//PPARA//PPARGC1A//PPP3CB//PPP3R2//PPP4R3B//PRKAA2//PRKACB//PRKAG3//SIK2//SLC2A1
hsa05213	Endometrial cancer	15	0.001151685	AKT1//APC2//AXIN1//BAD//BAK1//BRAF//CASP9//CCND1//GADD45B//GADD45G//GRB2//MYC//PDPK1//PIK3CD//TCF7
hsa04931	Insulin resistance	23	0.001282533	AKT1//CREB1//FOXO1//G6PC2//GFT2//IKKBK//IRS2//MLXIP//PDPK1//PIK3CD//PPARA//PPARGC1A//PPP1CA//PPP1CC//PPP1R3A//PRKAA2//PRKAG3//PRKCZ//PTPN1//RPS6KA2//RPS6KA3//RPS6KA6//SLC2A1
hsa05215	Prostate cancer	21	0.001649782	AKT1//BAD//BRAF//CASP9//CCND1//CHUK//CREB1//CREBBP//ERG//FOXO1//GRB2//HSP90AA1//IKKBK//PDGFA//PDGFB//PDGFD//PDPK1//PIK3CD//TCF7//TMPRSS2//ZEB1
hsa05221	Acute myeloid leukemia	16	0.001988947	AKT1//BAD//BRAF//CCND1//CHUK//CSF1R//DUSP6//FCGR1A//GRB2//IKKBK//KIT//MYC//PER2//PIK3CD//PPARD//TCF7

Appendix A. Supplementary data

Supplementary data to this article can be found online at <https://doi.org/10.1016/j.heliyon.2024.e30295>.

References

- [1] M. Conte, L. Petraglia, S. Cabaro, et al., Epicardial adipose tissue and cardiac arrhythmias: focus on atrial fibrillation, *Front. Cardiovasc. Med.* 9(2022), <https://doi.org/10.3389/fcvm.2022.932262>.
- [2] P.S. Cunha, S. Laranjo, J. Heijman, M.M. Oliveira, The atrium in atrial fibrillation – a clinical review on how to manage atrial fibrotic substrates, *Front. Cardiovasc. Med.* 9(2022), <https://doi.org/10.3389/fcvm.2022.879984>.
- [3] A. Hruby, F.B. Hu, The epidemiology of obesity: a big picture, *Pharmacoeconomics* 33 (7) (2015) 673–689, <https://doi.org/10.1007/s40273-014-0243-x>.
- [4] S.N. Hatem, A. Redheuil, E. Gandjbakhch, Cardiac adipose tissue and atrial fibrillation: the perils of adiposity, *Cardiovasc. Res.* 109 (4) (2016) 502–509, <https://doi.org/10.1093/cvr/cvw001>.
- [5] L. Zhao, D.L. Harrop, A. Ng, W. Wang, Epicardial adipose tissue is associated with left atrial dysfunction in people without obstructive coronary artery disease or atrial fibrillation, *Can. J. Cardiol.* 34 (8) (2018) 1019–1025, <https://doi.org/10.1016/j.cjca.2018.05.002>.
- [6] E.A. Orellana, E. Siegal, R.I. Gregory, Trna dysregulation and disease, *Nat. Rev. Genet.* (2022), <https://doi.org/10.1038/s41576-022-00501-9>.
- [7] X. Gu, Y. Zhang, X. Qin, S. Ma, Y. Huang, S. Ju, Transfer rna-derived small rna: an emerging small non-coding rna with key roles in cancer, *Exp. Hematol. Oncol.* 11 (1) (2022), <https://doi.org/10.1186/s40164-022-00290-1>.
- [8] E. Borek, B.S. Baliga, C.W. Gehrke, et al., High turnover rate of transfer rna in tumor tissue, *Cancer Res.* 37 (9) (1977) 3362–3366.
- [9] J. Du, T. Huang, Z. Zheng, S. Fang, H. Deng, K. Liu, Biological function and clinical application prospect of tsrnas in digestive system biology and pathology, *Cell Commun. Signal.* 21 (1) (2023) 302, <https://doi.org/10.1186/s12964-023-01341-8>.
- [10] N.T. Chiou, R. Kageyama, K.M. Ansel, Selective export into extracellular vesicles and function of trna fragments during t cell activation, *Cell Rep.* 25 (12) (2018) 3356–3370, <https://doi.org/10.1016/j.celrep.2018.11.073>.
- [11] K. Yang, Q. Xiao, K. Wang, et al., Circulating exosomal tsrnas: potential biomarkers for large artery atherosclerotic stroke superior to plasma tsrnas, *Clin. Transl. Med.* 13 (2) (2023), <https://doi.org/10.1002/ctm2.1194>.
- [12] S. Li, Z. Xu, J. Sheng, Trna-derived small rna: a novel regulatory small non-coding rna, *Genes* 9 (5) (2018), <https://doi.org/10.3390/genes9050246>.
- [13] N. Guzzi, C. Bellodi, Novel insights into the emerging roles of trna-derived fragments in mammalian development, *RNA Biol.* 17 (8) (2020) 1214–1222, <https://doi.org/10.1080/15476286.2020.1732694>.

- [14] L. Zhao, Z. Ma, Z. Guo, M. Zheng, K. Li, X. Yang, Analysis of long non-coding rna and mrna profiles in epicardial adipose tissue of patients with atrial fibrillation, *Biomed. Pharmacother.* 121(2020) 109634, <https://doi.org/10.1016/j.biopha.2019.109634>.
- [15] X. Yu, Y. Xie, S. Zhang, X. Song, B. Xiao, Z. Yan, Trna-derived fragments: mechanisms underlying their regulation of gene expression and potential applications as therapeutic targets in cancers and virus infections, *Theranostics* 11 (1) (2021) 461–469, <https://doi.org/10.7150/thno.51963>.
- [16] J. Zhou, S. Liu, Y. Chen, et al., Identification of two novel functional trna-derived fragments induced in response to respiratory syncytial virus infection, *J. Gen. Virol.* 98 (7) (2017) 1600–1610, <https://doi.org/10.1099/jgv.0.000852>.
- [17] W. Wu, E. Choi, B. Wang, et al., Changes of small non-coding rnas by severe acute respiratory syndrome coronavirus 2 infection, *Front. Mol. Biosci.* 9(2022), <https://doi.org/10.3389/fmolb.2022.821137>.
- [18] L. Tong, W. Zhang, B. Qu, et al., The trna-derived fragment-3017a promotes metastasis by inhibiting nell2 in human gastric cancer, *Front. Oncol.* 10(2021), <https://doi.org/10.3389/fonc.2020.570916>.
- [19] L.L. Zheng, W.L. Xu, S. Liu, et al., Trf2cancer: a web server to detect trna-derived small rna fragments (trfs) and their expression in multiple cancers, *Nucleic Acids Res.* 44 (W1) (2016) W185–W193, <https://doi.org/10.1093/nar/gkw414>.
- [20] Y. Fang, Y. Liu, Y. Yan, et al., Differential expression profiles and function predictions for trfs & tirmas in skin injury induced by ultraviolet irradiation, *Front. Cell Dev. Biol.* 9(2021), <https://doi.org/10.3389/fcell.2021.707572>.
- [21] W. Wu, I. Lee, H. Spratt, X. Fang, X. Bao, Trna-derived fragments in alzheimer's disease: implications for new disease biomarkers and neuropathological mechanisms, *J. Alzheim. Dis.* 79 (2) (2021) 793–806, <https://doi.org/10.3233/JAD-200917>.
- [22] Y. Zhang, L. Ren, X. Sun, et al., Angiogenin mediates paternal inflammation-induced metabolic disorders in offspring through sperm tsrnas, *Nat. Commun.* 12 (1) (2021), <https://doi.org/10.1038/s41467-021-26909-1>.
- [23] Z. Yang, P. Li, Z. Li, T. Tang, W. Liu, Y. Wang, Altered expression of transfer-rna-derived small rnas in human with rheumatic heart disease, *Front. Cardiovasc. Med.* 8(2021), <https://doi.org/10.3389/fcvm.2021.716716>.
- [24] R. Zhao, M. Ackers-Johnson, J. Stenzig, et al., Targeting chondroitin sulfate glycosaminoglycans to treat cardiac fibrosis in pathological remodeling, *Circulation* 137 (23) (2018) 2497–2513, <https://doi.org/10.1161/CIRCULATIONAHA.117.030353>.
- [25] A. Haryono, K. Ikeda, D.B. Nugroho, et al., Chgn-2 plays a cardioprotective role in heart failure caused by acute pressure overload, *J. Am. Heart Assoc.* 11 (7) (2022), <https://doi.org/10.1161/JAHA.121.023401>.
- [26] D. Tong, G.G. Schiattarella, N. Jiang, et al., Impaired amp-activated protein kinase signaling in heart failure with preserved ejection fraction–associated atrial fibrillation, *Circulation* 146 (1) (2022) 73–76, <https://doi.org/10.1161/CIRCULATIONAHA.121.058301>.
- [27] K.N. Su, Y. Ma, M. Cacheux, et al., Atrial amp-activated protein kinase is critical for prevention of dysregulation of electrical excitability and atrial fibrillation, *JCI Insight* 7 (8) (2022), <https://doi.org/10.1172/jci.insight.141213>.
- [28] Z. Wang, Y. Wang, Z. Liu, et al., Effect of insulin resistance on recurrence after radiofrequency catheter ablation in patients with atrial fibrillation, *Cardiovasc. Drugs Ther.* (2022), <https://doi.org/10.1007/s10557-022-07317-z>.